Finja Borowski*, Sebastian Kaule, Jan Oldenburg, Alper Öner, Klaus-Peter Schmitz, Michael Stiehm

In silico model to assess thrombosis risk of TAVR with hemodynamic predictors using fluid structure interaction

https://doi.org/10.1515/cdbme-2023-1125

Abstract: The promising results of transcatheter aortic valve replacement (TAVR) over the past two decades indicate an expansion of the patient cohort toward patients with intermediate or low surgical risk. Since some complications of TAVR have already been minimized, subclinical leaflet thrombosis (SLT) has gained importance in recent years. SLT is manifested by a thrombotic layer on the prosthetic leaflets that gradually reduces leaflet motion. The resulting decrease in functionality of the TAVR causes a need for re-intervention. The origin of SLT and approaches to prevent SLT are still unexplored. For this reason, we have developed an *in silico* model that can be used during the design development process of TAVR devices to estimate the thrombosis risk of the implant. Based on passive scalar transport, hemodynamic metrics are used to quantify platelet activation and aggregation which are associated with the formation of thrombosis. In conjunction with a numerical simulation model considering the fluid-structure interaction between the blood mimicking fluid and the TAVR implanted in an aortic root, the thrombosis risk can be modeled. The simulation model can be used to calculate the three-dimensional flow structures within the native sinus and neo-sinus and also provides the ability to derive metrics to assess the risk of thrombosis. We demonstrated that this *in silico* model is a time-effective tool to assess thrombosis risk in TAVR product development.

Keywords: transcatheter aortic valve replacement, thrombosis risk, fluid structure interaction

***Corresponding author: Finja Borowski:** Institute of ImplantTechnology and Biomaterials, Friedrich-Barnewitz-Straße 4, Rostock, Germany, e-mail: finja.borowski@iib-ev.de
Sebastian Kaule, Jan Oldenburg, Klaus-Peter Schmitz, Michael Stiehm: Institute of ImplantTechnology and Biomaterials, Rostock, Germany
Alper Öner: Department of Cardiology Rostock University Medical Center, Rostock, Germany

1 Introduction

Transcatheter aortic valve replacement (TAVR) is meanwhile an established therapy for the treatment of severe aortic valve stenosis approved in all risk categories. Since the method has been used in clinical practice, some adverse events have occurred after therapy with a TAVR, such as increased pressure gradient in a patient-TAVR mismatch, coronary obstruction, paravalvular leakage or annulus rupture [1]. These events occur immediately after implantation of a TAVR and, depending on their severity, affect the functionality of TAVR.

In the recent past, the appearance of valve thrombosis (VT) has been noted. VT does not occur immediately after implantation rather it is a continuous ongoing process that leads to pathological alteration, especially of the TAVR leaflets, gradually impairing its functionality and increasing the risk of embolic events.

Accumulation of a thrombotic layer on prosthetic leaflets leads to hypoattenuating leaflet thickening (HALT), which results in reduced leaflet motion. If this process is not treated by anticoagulation, the transvalvular pressure gradient increases and the durability of the TAVR will decrease [2].

The SAVORY and RESOLVE register, established to study subclinical leaflet thrombosis (SLT), demonstrate that the incidence of HALT is significantly more frequent 30 days after TAVR implantation than with surgical aortic valve replacement (SAVR) (13.3% TAVR vs. 5.0% SAVR, p=0,03) [3,4].

The formation of a thrombotic layer has been associated with hemodynamic properties such as blood stagnation or increased shear rate in literature, as summarized by Cito et al. (2013) [5]. Pathologically high shear rates in blood flow favour platelet activation [6]. If activated platelets pass into blood stagnation areas, adhesion of blood components to biomaterial surfaces can be observed [6].

The development of predictive models of leaflet thrombosis has often focused on the application of patient-specific data to facilitate in clinical application and planning. Nevertheless,

thrombosis is also of great importance in the development process of innovative TAVR.
The ISO 5840 (2021) also included evidence about the thrombotic potential of TAVR for the first time. The standard recommends a combined model of *in vitro* studies and *in silico* simulations, but not further specified. Therefore we attempted to develop an assessment model for thrombosis risk of TAVR that can be used in regulatory evidence as well as in simulations of clinical applications.

2 Materials and methods

2.1 Thrombosis risk assessment model

Due to the numerous sub-processes that lead to the development of thrombosis, the complete thrombotic cascade is too computationally expensive to be completely simulated in complex geometries and flow fields. Therefore a macroscopic continuum model was used to consider important hemodynamic sub-aspects of thrombosis.
Platelet activation was modelled with a scalar transport equation based on a cumulated linear stress-exposure-time model as proposed by Hansen et al. (2015) for use in aneurysm flow [7]. The scalar metric SIPA (shear induced platelet activation) corresponds to the activation level of the fluid, which is temporally (t) and spatially $\vec{x}(x, y, z)$ influenced by a convection flow through the flow velocity $\vec{u}(\vec{x}, t)$ and a diffusion flow with the diffusion coefficient D:

$$\frac{dSIPA(\vec{x},t)}{dt} + \vec{u}(\vec{x},t) \cdot \nabla SIPA(\vec{x},t) = -D \cdot \nabla^2 SIPA(\vec{x},t) + \tau(\vec{x},t) \qquad (1)$$

The activation indication is done by the source term in which the spatial and temporal distribution of the shear stress $\tau(\vec{x}, t)$ is considered in the equation. However, the scalar value is not intended as a metric for estimating the activated or non-activated state, but rather to identify areas of fluid with higher shear history and is intended to be a metric to compare different TAVR designs and configurations.
The influence of stagnation and recirculation areas favouring platelet adhesion to surfaces is quantified by blood residence time (BRT) based on the publication by Ghirelli and Leckner [8], the BRT is also defined by a passive scalar transport:

$$\frac{\partial BRT(\vec{x},t)}{\partial t} + \vec{u}(\vec{x},t) \cdot \nabla BRT(\vec{x},t)) = -D \cdot \nabla^2 BRT(\vec{x},t) + 1 \qquad (2)$$

The approach of residence time in relation to the washout behaviour of TAVR has already been published by our working group [9] and has now been enhanced by an equation for shear-induced impact on thrombosis risk.

2.2 Fluid structure interaction (FSI) simulation

Computational domain
The Geometry is composed of an aortic root model and a simplified model of the TAVR. The geometry of the aortic root has already been published in *in vitro* studies from our working group and is consistent with the *in silico* studies we performed. The aortic root model was first published in Borowski et al. [10] and has been continuously refined through retrospective analysis of patient data and regulatory requirements [11]. The TAVR model consists of the artificial leaflets and a skirt. The TAVR stent is neglected.

Material properties, discretization and coupling
The vessel walls were assumed to be rigid. The material properties of the artificial leaflets depend on the material used, which is why different material properties apply to different TAVR. Although pericardial tissue exhibits anisotropic and hyperelastic properties, linear-elastic behaviour is often assumed in complex simulations. We also considered a linear elastic material model for the leaflets (E = 1 MPa, ν = 0.46, ρ = 1100 kg/m^3). The fluid was modelled as an incompressible, non-Newtonian fluid. The shear-dependent character of the blood was replicated using the Carreau-Yasuda model with parameter values from Cho and Kensey [12].
The fluid and the structure environment were meshed separately. A uniform cell size for both domains was used only at the interaction surface. This type of meshing is possible due to the partitioned implicit coupling algorithm of the FSI simulation. A mesh independence test was performed for both meshes. The dynamic mesh adaption of the fluid domain was implemented using the Arbitrary-Lagrangian-Eulerian (ALE) approach with a diffusion based smoothing function.
As the Reynolds number of blood flow in the ascending aorta reaches values above Re = 5000, a SST-k-ω turbulence model was used. To reduce the computational effort, one leaflet was simulated and symmetry conditions were assumed with respect to the other two leaflets. The contact between the leaflets was established with a rigid contact model. For the stent frame, a cylindrical contact model was also added to the structural simulation. To ensure mesh adaptation with the ALE method, a small gap was added between the contact tool and the symmetry plane of the fluid.

Boundary conditions
The flow-inducing boundary condition was a velocity boundary condition at the inlet based on experimentally determined data from a hydrodynamic circulation model that mimics (patho-)physiological flow conditions in the left heart. To generate a time-dependent average velocity calculated from the

flow rate measurement, clinical parameters were set, which are listed in Table 1.

Tab. 1: Clinical parameter used to mimic physiological flow conditions as boundary condition.

clinical parameter	
heart rate	70 bpm
mean aortic pressure	100 mmHg ± 2 mmHg
systolic duration	35 % ± 5 %
fluid temperature	37°C ± 2°C
cardiac output	3,5 l/min

We divided the simulation model into three sub-models caused by the different boundary conditions during a cardiac cycle: **I** diastolic pressure load, **II** systolic flow and **III** diastolic flow, see fig. 1.

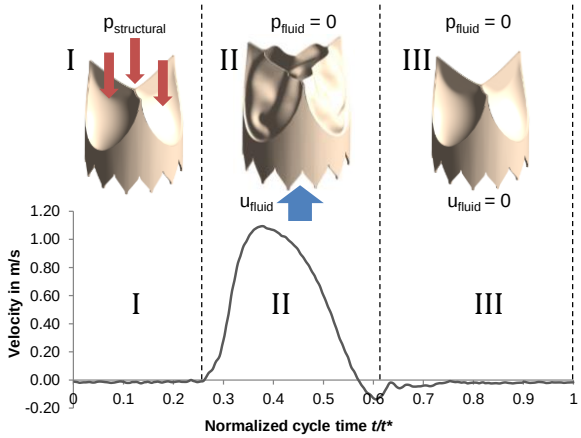

Figure 1: Boundary conditions of the simulation model divided into three sub-models,, I) diastolic pressure load, II) systolic flow and III) diastolic flow.

In the first step, diastolic pressure is applied normally to the leaflet to generate initial normal and shear stresses. After that, the actual FSI simulation begins. The flow velocity at the inlet is specified and a bidirectional force and displacement transfer is performed at the interaction surface. An inlet velocity of $u = 0$ is defined during diastolic flow.

The scalar transport equations for calculating thrombosis metrics were implemented in the equations to be solved. The FSI simulation was performed using ANSYS 18.0 (ANSYS Corp., Canonsburg, USA).

3 Results and discussion

The result of the FSI simulation is the transient velocity field in the vicinity of a TAVR. Some exemplary results of the velocity field at three time points of a cardiac cycle (peak systole, start of diastole, and end of diastole) are shown in Figure 2.

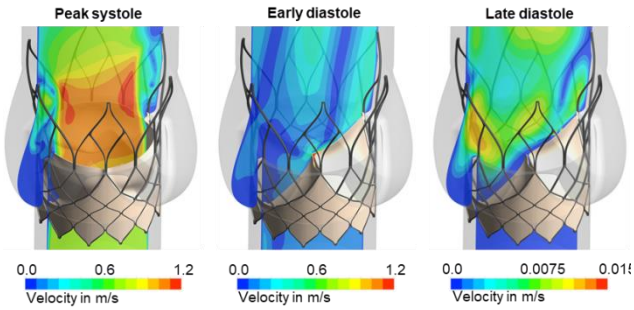

Figure 2: Longitudinal section of the simulated velocity field during peak systole, early diastole, and late diastole.

Simultaneously with the calculation of the velocity field, the passive transport equations for the SIPA und BRT were calculated. The resulting spatial distribution of BRT and SIPA after one cardiac cycle is shown in Figure 3.

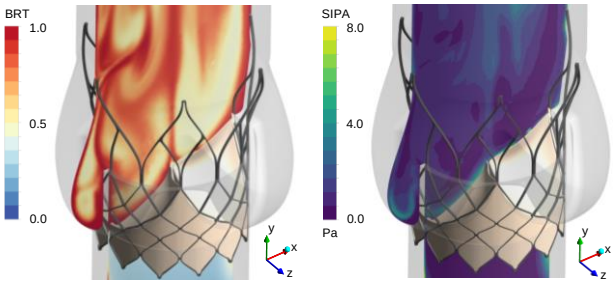

Figure 3: Exemplary plot of BRT and SIPA in the z=0 plane of a TAVR at late diastole.

A region of interest (ROI) was defined for the evaluation of thrombosis risk, based on the local occurrence of HALT restricted to the neo-sinus region, see Fig. 4. The ROI is limited by the basal attachments of the artificial leaflets and the cross-section directly distal to the artificial leaflets.

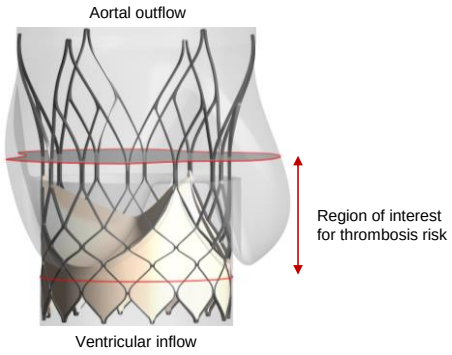

Figure 4: Region of interest in the area of the native sinus and the newly formed neo-sinus between the calcified native leaflets and the artificial leaflets.

As comparative values for platelet activation, a histogram of SIPA thresholds was plotted showing the percentage of fluid volume within a range of accumulated shear stress values relative to the fluid volume of the ROI, see Fig. 5. The histogram shows the size of the area with increased shear stress (6-8 Pa).

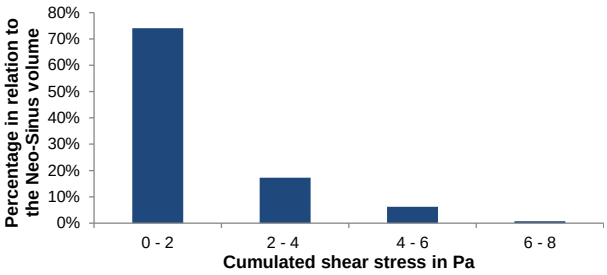

Figure 5: Volume fraction of SIPA thresholds relative to the total volume in native and neo sinus.

The second comparative metric considered for thrombosis assessment is the area of high blood residence time. For comparability of, e.g. different heart rates resulting in different physical time durations, the BRT was normalized to the time duration of one heart cycle. In this way, the normalized BRT ranges between a value of 0 and 1 regardless to the duration of a cardiac cycle. The histogram of BRT distribution is shown in Fig. 6 for the defined ROI.

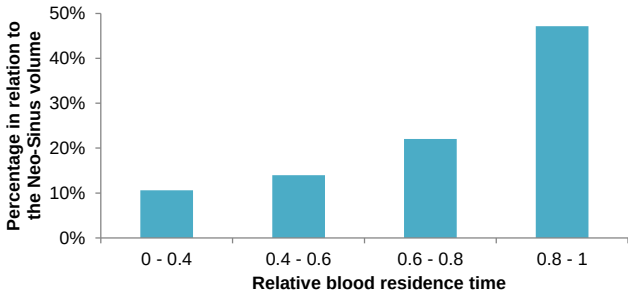

Figure 6: Volume fraction of BRT thresholds relative to the total volume in native and neo sinus.

Using the volume distribution of both metrics, the region of increased shear stress and high blood residence time can be comparatively analyzed.

A more commonly published approach to assess the thrombosis risk of TAVR is a Lagrangian approach, in which a discrete number of particles are dispersed in an ROI, as shown, for example, by Midha et al. [13]. However, this approach requires the calculation of individual particle trajectories and is significantly dependent on the initial number and localization of particles.

With the scalar transport approach for the thrombosis metrics that we demonstrated in this study, the equations to be calculated are computed simultaneously with the Navier-Stokes equations of the flow field. Because of the resulting lower computational effort and independence from an initial particle distribution, the presented method can be suggested as an effective and robust tool for the assessment of thrombosis risk of TAVR.

Author Statement

Research funding: This project has received funding from the European Union's Horizon 2020 research and innovation program under grant agreement No 101017578. The EU is not responsible for any use that may be made of the results shown in this publication or any information contained therein.

References

[1] Mas-Peiro S, Fichtlscherer S, Walther C et al. Current issues in transcatheter aortic valve replacement. Journal of thoracic disease 2020;4:1665-1680.

[2] Garcia S, Fukui M, Dworak M, et al. Clinical impact of hypo-attenuating leaflet thickening after transcatheter aortic valve replacement. Circulation: Cardiovascular Interventions, 2022:15(3), e011480.

[3] Chakravarty T, Sondergaard L, Friedman J, et al. Subclinical leaflet thrombosis in surgical and transcatheter bioprosthetic valves: an observational study. The Lancet 2017;10087:2383-2392.

[4] Makkar R, Blanke P, Leipsic J, et al. Subclinical leaflet thrombosis in transcatheter and surgical bioprosthetic valves. Journal of the American College of Cardiology 2020;24:3003-3015.

[5] Cito S, Mazzeo M, Badimon L. A review of macroscopic thrombus modeling methods. Thrombosis research 2013;2:116-124.

[6] Anand M, Rajagopal K, Rajagopal KR. A Model Incorporating some of the Mechanical and Biochemical Factors Underlying Clot Formation and Dissolution in Flowing Blood. Journal of Theoretical Medicine 2003;5(3-4):183-218.

[7] Hansen K, Arzani A, Shadden S. Mechanical platelet activation potential in abdominal aortic aneurysm. Journal of Biomechanical Engineering 2015;137:1-8.

[8] Ghirelli F, Leckner B. Transport equation for local residence time of a fluid. Chemical Engineering Science 2004;3:513-523.

[9] Stiehm M, Borowski F, Kaule S, et al. Computational flow analysis of the washout of an aortic valve by means of Eulerian transport equation. Current Directions in Biomedical Engineering 2019;5(1):123-126.

[10] Borowski F, Sämann M, Pfensig S, et al. Fluid-structure interaction of heart valve dynamics in comparison to finite-element analysis. Current Directions in Biomedical Engineering 2018;4(1):259-262.

[11] Borowski F, Kaule S, Oldenburg J, et al. Particle-Image-Velocimetry zur strömungsmechanischen Analyse des thrombogenen Potentials von Transkatheter-Aortenklappenprothesen. tm – Technisches Messen 2022;89(3):189-200.

[12] Cho Y, Kensey K. Effect of non-Newtonian viscosity of blood on flows in a diseases arterial vessel. Part 1: Steady flows. Biorheology 1991;28.3-4:241-262.

[13] Midha P, Raghav V, Okafor I, et al. The Effect of Valve-in-Valve Implantation Height on Sinus Flow. Annals of Biomedical Engineering. Annals of Biomedical Enginnering 2017;45(2):405-412.